

AUTOMATIC SATELLITE TRACKING SYSTEM
FOR THE
NASA SATELLITE PHOTOMETRIC OBSERVATORY

by

Glenn H. Mucklow

Optical Society of America
Florida Section Fall Meeting
September 20, 1980

(PREFACE-1M-105-17) AUTOMATIC SATELLITE
TRACKING SYSTEM FOR THE NASA SATELLITE
PHOTOMETRIC OBSERVATORY (NASA) 34

091-5119+

CCCL 22A

Unclass

05/12 0037440

ABSTRACT

The development of an Automatic TV Tracking System for NASA's mobile 61 cm aperture Satellite Photometric Observatory is described in this paper. The analysis techniques used to match the sensor FOV and resolutions to changing seeing conditions are covered in detail. Theoretical reasons for such matching of general interest are discussed. It is shown that the energy density in a satellite image is 11 times greater during good seeing conditions than during typical seeing conditions. The Z7987 image tube is shown to be able to detect 16th magnitude objects under ideal seeing conditions using only 8% of the light collected by the main telescope. Experimental results show that the SPO equipped with a Z7987 camera can track a satellite at any orbital velocity with less than 0.14 mr accuracy using the DBA Series 606 TV Tracker. The manual system used prior to the installation of the Automatic TV Tracking System could maintain track at 1.1 mr accuracy for comparison.

Figures

1. NASA Satellite Photometric Observatory (SPO)
2. Satellite Photometric Observatory Control Room
3. Sun/Satellite/Observer Geometry
4. Z7987 Camera Head on SPO Telescope
5. Resolution and Signal-to-Noise vs Light Level - Z7987
6. Comparison of Image Expansion and Halo Characteristics

Contents

INTRODUCTION

SPO TELESCOPE

ELECTRO-OPTICAL INTERFACE

Sensor FOV

Resolution

Sensor Requirements

SENSOR SELECTION

Sensor/SPO Performance

Blooming

ELECTRO-OPTICAL INTERFACE: RATIONALE

TELEVISION TRACKING

Centroid Tracking

Servo Interface

TRACKING EXPERIMENTS

CONCLUSION

ACKNOWLEDGEMENTS

Introduction

The mobile NASA Satellite Photometric Observatory (SPO) is used in a Langley program to determine the vertical distribution of stratospheric ozone from observations of eclipsing satellites. Stratospheric ozone, because of its strong absorption of solar ultraviolet radiation, is the primary heat source of the upper atmosphere. The eclipse technique consists of photometrically observing a satellite as it approaches the earth's shadow. The measured attenuation of satellite brightness due to absorption allows the determination of the vertical distribution of ozone. The technique has been successfully used to measure ozone concentrations from 15 to 50 kilometers.

The SPO, specifically designed for satellite photometry, originally used a manual system for the tracking of target satellites. The manual system, which required a 1.1 mr angular aperture and small guide telescope, limits the inherent detection capabilities of the SPO. The 1.1 mr angular aperture, while accommodating the positional errors associated with manual tracking, results in a large sky foreground component which in turn limits the system signal-to-noise ratio and detection levels. The small guide telescope, while providing a large field of view for the observer, limits the efficiency with which the satellite can be tracked.

The installation of the automatic satellite tracking system, which uses a .14mr aperture and the main telescope, provides a number of advantages. The smaller angular aperture greatly improves the system accuracy by reducing the sky foreground by a factor of 64. Since the signal-to-noise ratio is improved, and since the main

telescope will be used for tracking, fainter satellites may be acquired and detected. For example, the number of potential satellites for ozone observations has increased from 6 to over 25. The new system also provides continuous tracking, which insures that satellite data will be obtained during the critical period when the satellite enters the earth's shadow. Continuous data should improve the accuracy and resolution of the deduced ozone concentrations. In addition, manpower requirements could be reduced by one-quarter during a satellite tracking mission. The overall improved capabilities should permit the SPO to be used in new areas of space research, such as planetary atmospheres, asteroid physics, and atmospheric environmental studies using the NASA Space Shuttle.

SPO Telescope

The main instrument on the SPO is a 61 cm aperture astronomical telescope with a 12.2 m Cassegrain focal length. The instrument package consists of four thermoelectrically cooled photomultiplier tubes which may be configured for a variety of simultaneous multispectral measurements including polarimetric.

The scale factor of the telescope may be calculated as follows from the familiar FOV equation:

$$\begin{aligned} \tan \frac{\alpha}{2} &= \frac{W}{2F} & (1) \\ &= \frac{1 \text{ mm}}{2 (12.2 \times 10^3 \text{ mm})} \\ \frac{\alpha}{2} &= 41 \mu\text{r} \\ \alpha &= 82 \mu\text{r} \end{aligned}$$

and the scale factor is 82 microradians per millimeter where W is one millimeter in the image plane, F is the focal length, and α is the angular field of view of W .

The instrument package has a fixed 17.5 mm high focal plane stop with an aperture wheel containing 1.1, 0.6, 0.3, and 0.14 mr apertures. The telescope is positioned by a four axis mount which is mounted on a truck (Fig. 1) containing the control room (Fig. 2). Therefore, the telescope may track any satellite orbit from any location. A computer program at NASA Langley provides the four axis settings for a variety of locations and satellites.

Three guide telescopes with fields of view of several milliradians are used for manual acquisition and tracking. The observer guides the telescope on the satellite using a small portable stiffstick remote control while observing the satellite through a guide telescope. Three guide telescopes are used because observer access to certain guide telescope positions can be limited in some orientations of the four axis mount. Radiometric measurements are made as the satellite enters the earth's shadow as shown in Figure 3. Methods for accurately determining ozone concentrations from this data have been reported elsewhere. (Reference 1)

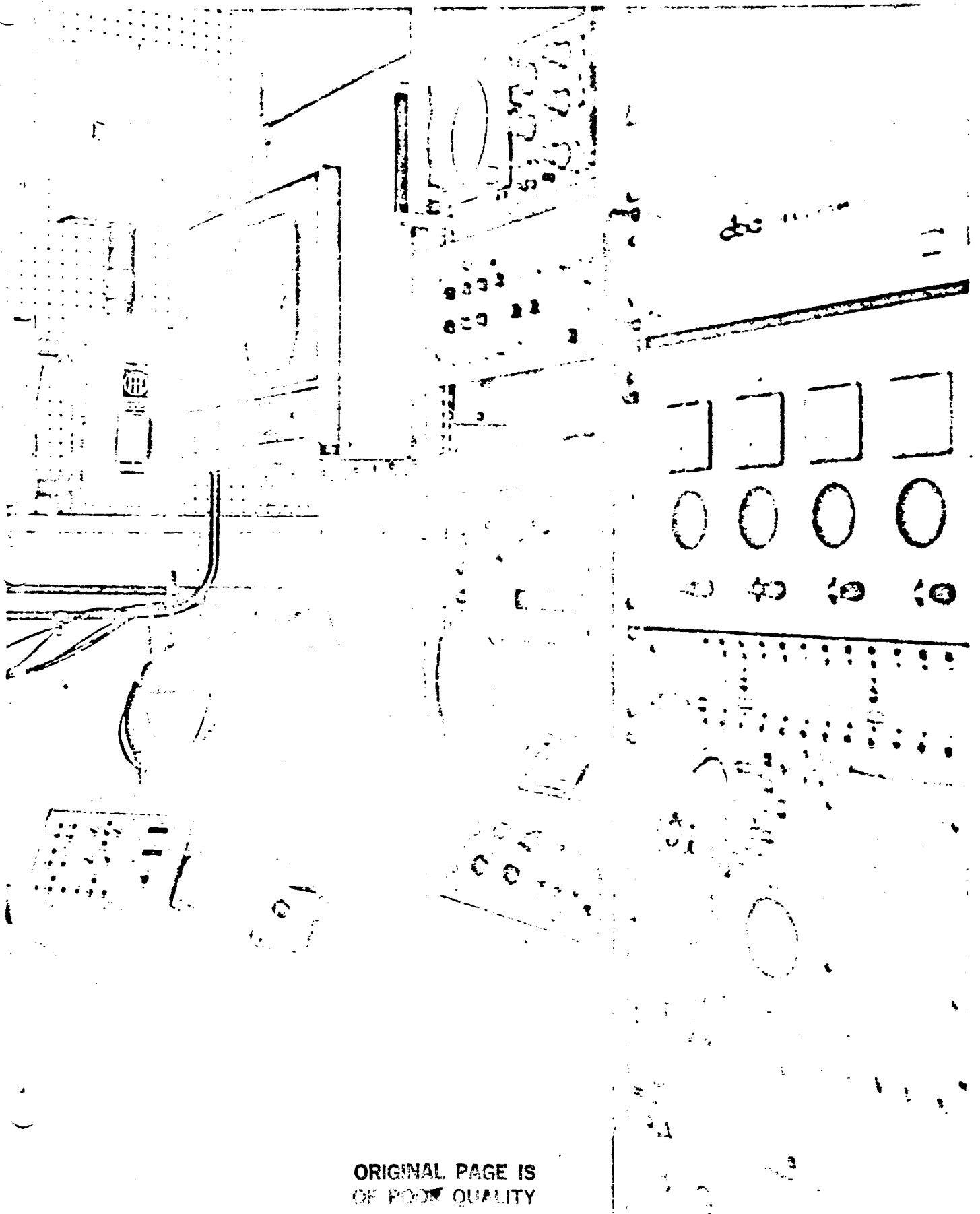
Optical Interface

An alternate focal plane for the automatic tracking sensor had to be located such that no interference with the existing or future instrument packages would occur. A separate guide telescope for the sensor was rejected due to potential alignment problems under the conditions in which the SPO operates, and the lack of a standard unit with sufficient focal length. A design was developed which located a low reflectivity



STANDARD PHOTOGRAPHY
1000 10th St. N.W.
WASHINGTON, D.C. 20004

FIGURE 2



ORIGINAL PAGE IS
OF POOR QUALITY

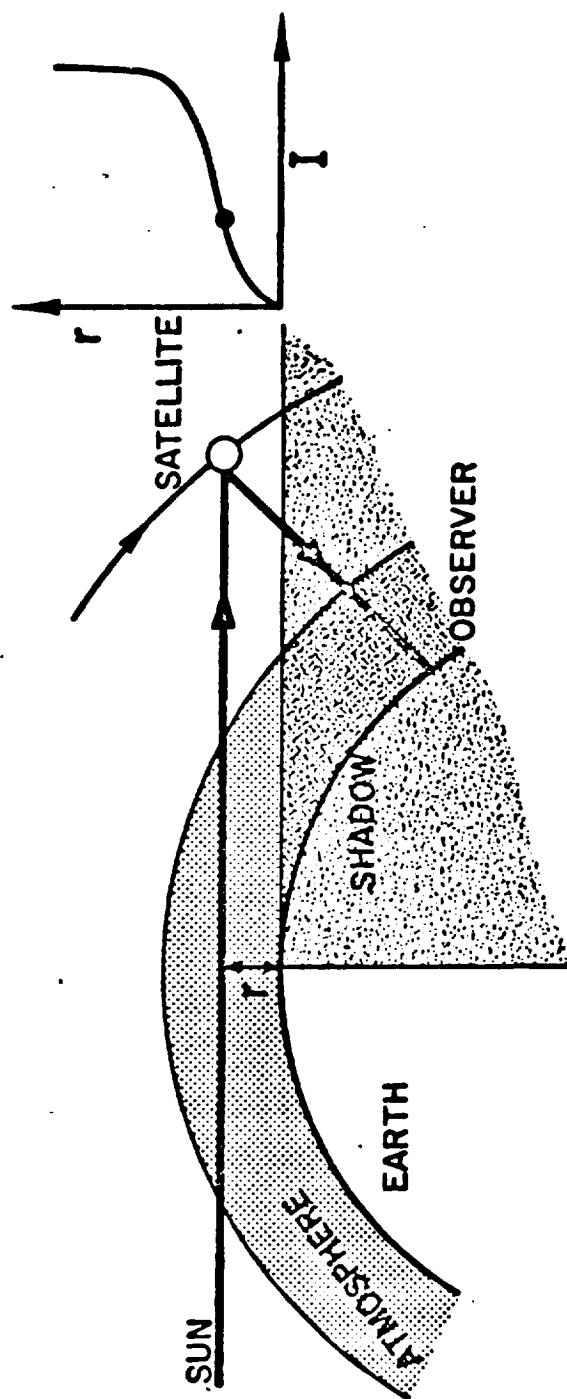
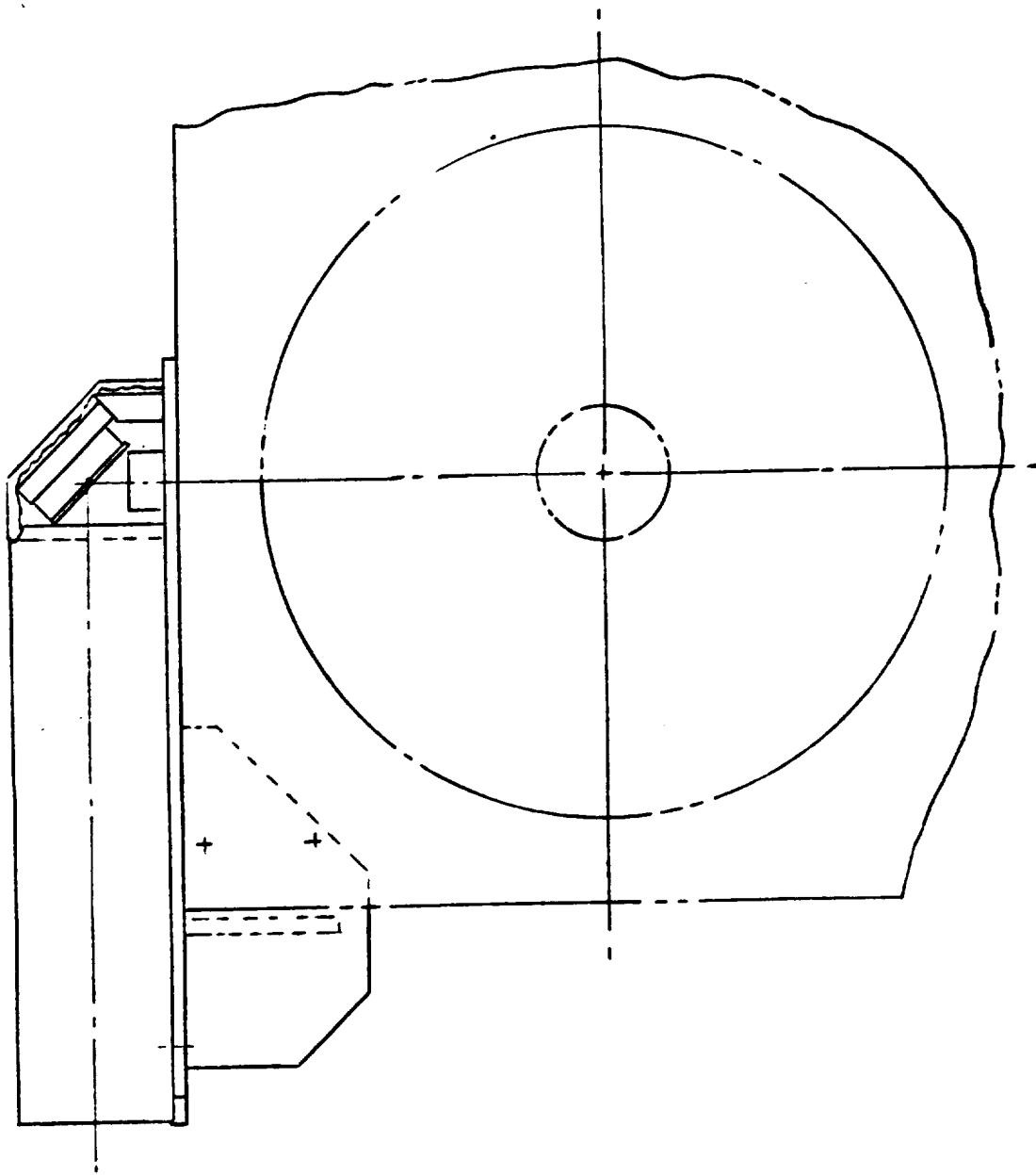


Figure 3 - Schematic diagram of sun-satellite-observer geometry and horizontal attenuation at tangential altitude r .



CAMERA HEAD ON SPO TELESCOPE

FIGURE 4

beam splitter in front of the primary mirror to reflect the target image to an alternate focal plane located on top of the main telescope as shown in Figure 4. This location eliminates any mechanical interference with an instrument package located at the normal Cassegrain focus.

Sensor FOV

The format of the sensor may be determined by consideration of field of view and resolution requirements. Seeing conditions through the atmosphere usually limit resolution at standard television frame rates of 30 frames per second. Resolution may be less than $5 \mu r$ during ideal seeing conditions to over $15 \mu r$ during typical seeing conditions. However, reported values do vary widely in the literature.

The focal plane stop in the instrument package is almost 1.5 mr vertically. This value is within a trained observer's manual satellite acquisition capability using the guide telescopes and would include any angular aperture which might be used behind the focal plane stop in the future also. Thus, the desired sensor field of view using an EIA standard 4:3 aspect ratio is 1.5 mr by 2 mr.

Resolution

The limiting vertical resolution for a raster scan system is the number of active horizontal scan lines divided by the square root of two (Reference 2). This results in a vertical resolution of approximately 340 TV lines per raster height for a standard 525 line system after subtracting the inactive lines during retrace between fields. Upon dividing this into the desired 1.5 mr vertical field of view, the angular resolution becomes $4.4 \mu r$ per TV line vertically. This value corresponds well with good seeing

conditions of approximately $5 \mu\text{r}$ resolution. Hence, a standard 525 line system is adequate. The horizontal resolution factor for an EIA standard 525 line, 30 frame per second system is 80 TVL/MHz. Therefore, the horizontal resolution will be equal to the vertical resolution at a bandwidth of 4.25 MHz. Other scan formats may be optimum during certain conditions (Reference 3) and the tracking sensor has the capability of instantly switching to any one of three preset formats. In addition, two modes of operation are available in the DBA Series 606 tracker used to process the sensor signal and guide the telescope. Either single pixel targets may be detected or a correlation mode may be selected as a method of noise discrimination such that the target must subtend several pixels to be detected. A four TV line target would correspond well to typical seeing conditions of approximately $15 \mu\text{r}$ resolution.

Sensor Requirements

Extending the stellar magnitude tracking capability of the SPO to 9th magnitude increases the number of potential satellite targets from 6 to over 25. However, the instrument package can operate down to 12th magnitude for certain measurements. Hence, the desired sensitivity requirement of the sensor is the flux at the sensor focal plane from a 12th magnitude star.

Modern photoemissive (S-25) surfaces cover the spectral range from less than $0.4 \mu\text{m}$ to over $0.8 \mu\text{m}$. A 0.0 magnitude star of the G2 spectral class provides about $4 \times 10^{-12} \text{ W cm}^{-2} \text{ micrometer}^{-1}$ at the earth's surface. However, sensor data is usually normalized to a 2854 K light source which is closer to a M5 spectral class. The bolometric correction for an M5 star is -2.48 compared to the G2 star above. Thus,

$4 \times 10^{-12} \text{ W cm}^{-2} \mu\text{m}^{-1}$ corresponds to the flux from a 2.5 magnitude star at the sensor's optical system for comparison with sensor data. A difference of one stellar magnitude is a factor of 2.512. Hence, the ratio between a 2.5 magnitude star and a 12th magnitude star is

$$2.512^{(2.5-12)} = 1.6 \times 10^{-4} \quad (2)$$

and the flux from a 12th magnitude star over the sensor's 0.4 to 0.8 μm spectral range is

$$\begin{aligned} (4 \times 10^{-12} \text{ W cm}^{-2} \mu\text{m}^{-1}) (1.6 \times 10^{-4}) (0.4 \mu\text{m}) \\ = 2.5 \times 10^{-16} \text{ W cm}^{-2} \end{aligned} \quad (3)$$

at the SPO telescope aperture.

It has been shown above that the seeing limited resolution is matched to the limiting resolution of a standard 525 line TV system at 4.4 μr during ideal seeing conditions. Since the scale factor of the SPO telescope is 82 $\mu\text{r/mm}$, one pixel becomes

$$(4.4 \mu\text{r})^2 (82 \mu\text{r/mm})^{-2} = 2.9 \times 10^{-3} \text{ mm}^2 \quad (4)$$

in the focal plane of the sensor. The transmission through the telescope optics via reflection from the beam splitter allows 8% of the energy collected by the 61 cm telescope aperture to be focused into the star image. The optical gain of the telescope for a point source may be defined as the ratio of the aperture area to the image area. This becomes

$$(305 \text{ mm})^2 (2.9 \times 10^{-3} \text{ mm}^2)^{-1} = 3.2 \times 10^7 \quad (5)$$

during ideal seeing conditions. The image area increases to

$$(15 \mu r)^2 (82 \mu r/mm)^{-2} = 3.3 \times 10^{-2} mm^2 \quad (6)$$

during typical seeing conditions and the optical gain is reduced to

$$(305 mm)^2 (3.3 \times 10^{-2} mm^2)^{-1} = 2.8 \times 10^6. \quad (7)$$

Thus, the energy density of a 12th magnitude star in the sensor focal plane is

$$(2.5 \times 10^{-16} W cm^{-2}) (2.8 \times 10^6) (.08) = 5.6 \times 10^{-11} W cm^{-2} \quad (8)$$

or $5.6 \times 10^{-7} W m^{-2}$. This may be converted to photometric units using a conversion factor of 20 lumens/watt for a 2854 K light source. Thus, the desired sensor sensitivity is 1.1×10^{-5} lumens/ m^2 (LUX). This represents a slightly conservative estimate since the satellite targets will be illuminated by sunlight which is closer to a 5500 K light source. The responsivity of a typical S-25 surface is almost four times higher for sunlight than for the 2854 K source used in these calculations. The format size in the focal plane for a 1.5 mr x 2.0 mr FOV is calculated from the scale factor of 82 $\mu r/mm$ to be 19 mm x 25 mm.

Sensor Selection

The literature contains a great deal of data on the different performance characteristics of image sensors (Reference 4,5, etc.). One image tube used for astronomical applications is the G.E. Z-7987. This tube has the unique combination of S-25 photocathode and a thin film Mg O target providing up to 100 times the sensitivity of an image isocon. The performance characteristics of this tube have

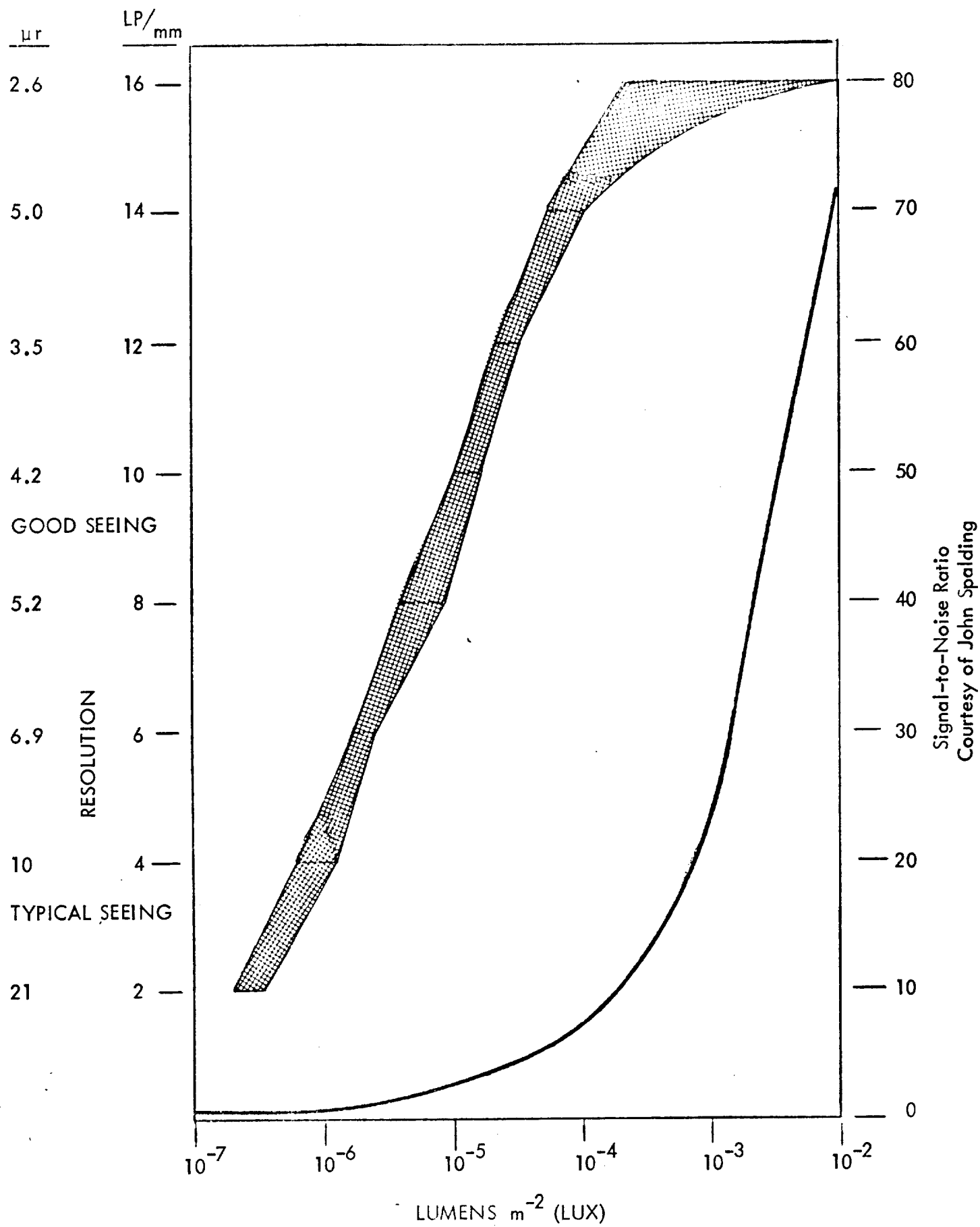


FIGURE 5

been reported elsewhere (Reference 6) and will not be covered here. Gurski and Spalding have reported comparing an unintensified G.E. 7987 camera with a Westinghouse WL-31792 EBS tube coupled to a WL-30677 intensifier and with a slow scan SIT camera. The 4 meter aperture telescope at Kitt Peak National Observatory was used for these experiments which were conducted on the same night during seeing conditions of 12 - 15 μ r resolution. The Z-7987 was reported to be superior to either of the other cameras (Reference 7).

Sensor/SPO Performance

The Z-7987 is an image orthicon camera type which becomes signal-to-noise limited by noise in the scanning electron beam at normal light levels. Figure 5 shows the resolution and theoretical signal-to-noise performance of the Z-7987 image tube as a function of light level. The signal-to-noise ratio is for a single frame at 10 MHz bandwidth based on beam current being optimized at each light level. It may be seen from the graph that the Z-7987 sensor is capable of detecting 10^{-5} LUX targets at resolution required during good seeing conditions. It was shown above that the gain of the SPO optical system is over 11 times better under ideal seeing conditions than typical seeing conditions. Therefore, since 10^{-5} LUX represents a 12th magnitude body under typical seeing conditions, it represents better than a 16th magnitude body during ideal seeing conditions. Next, considering the optical gain and image size stated above for typical seeing, the graph shows that the sensor is capable of detecting 15th magnitude bodies at 6.9×10^{-7} LUX during typical seeing conditions. However, the signal-to-noise ratio at this light level would require electronics to operate in the

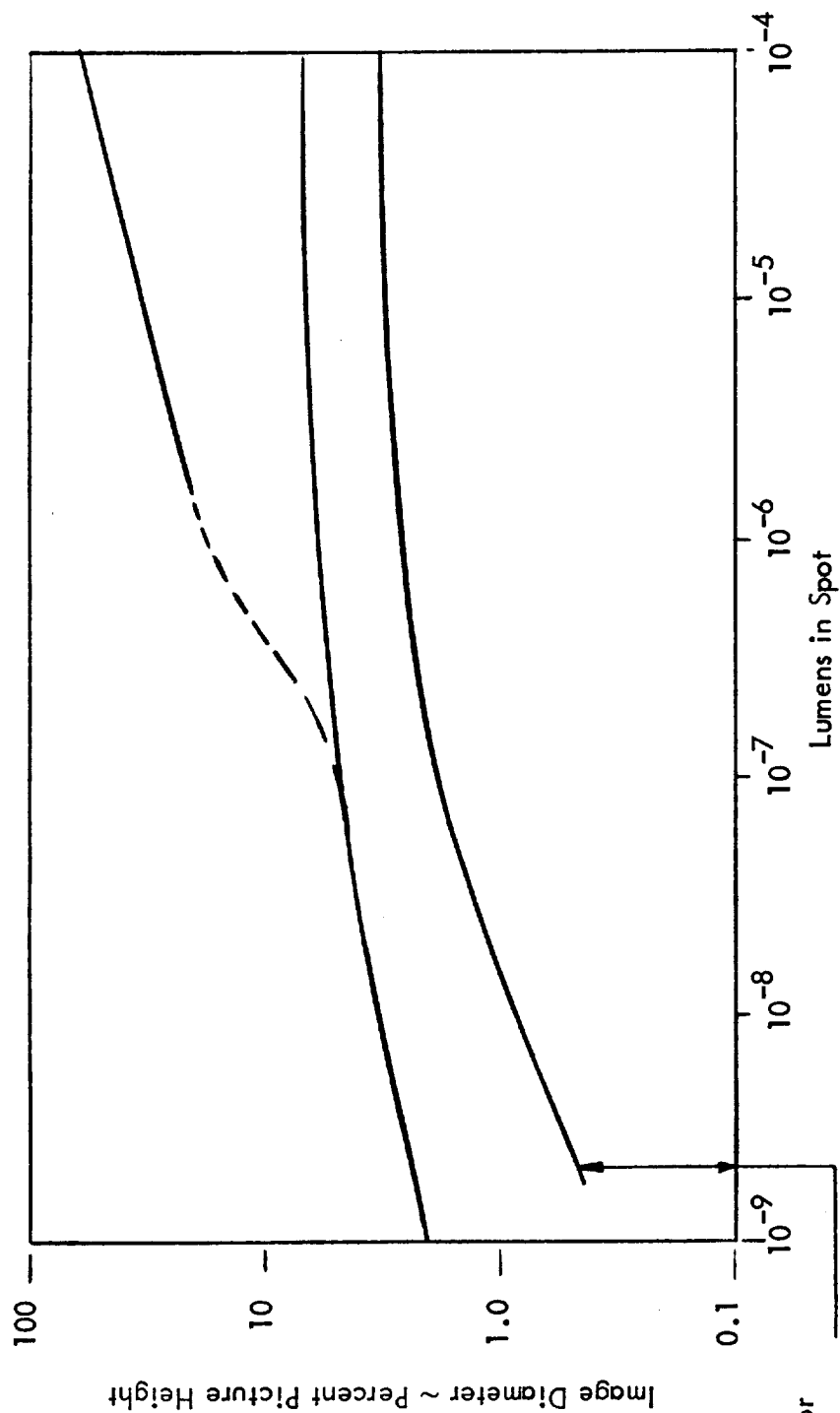
area correlation mode mentioned above. The integration and correlation capability of the human eye/brain combination enables the observer to detect targets at fractional signal-to-noise levels on a TV monitor. Even allowing for moderate degradation, it would seem reasonable that the Z-7987 sensor can detect the required 12th magnitude body at a signal-to-noise ratio of 2:1 which is ample for electronic centroid tracking (Reference 8).

Blooming

A blooming problem unique to the SPO results from the requirement to track satellites as they enter the earth's shadow. A sun illuminated PAGEOS satellite can represent a 2nd magnitude image before entering the shadow (Reference 9) and then drop several magnitudes in a matter of seconds. The Z-7987 exhibits a minimum of blooming or halo when saturated as shown in Figure 6. Thus, the sensor may be optimized for tracking the satellite into the earth's shadow and allowed to saturate during acquisition and tracking before entering the shadow.

Electro-Optical Interface: Rationale

The preceding methods of matching the seeing limited optical resolution to the sensor's pixel size apply in general to astronomical systems. The importance of this matching must be emphasized, especially for sky foreground limited conditions. If the seeing limited image of the star or satellite is smaller than the sensor's pixel size, the image and several elements of sky foreground flux will be summed in the single pixel, thereby reducing the image signal-to-sky foreground noise ratio. On the other hand, if the image extends over several sensor pixels the energy density of



Beam Setup for
Discharge of
Highlight Signal

COMPARISON OF IMAGE EXPANSION AND HALO CHARACTERISTICS

FIGURE 6

the image is reduced, thereby reducing the image signal-to-electronic noise level. Optimum sensor response occurs when the seeing limited optical resolution element exactly fills the sensor pixel size.

As stated previously, the SPO tracking camera is capable of switching between three preset format sizes to match seeing conditions. A continuously variable zoom intensifier would have enabled exact matching of sensor resolution with varying seeing conditions and resulted in sensitivity limited by photon statistics. However, the zoom intensifier was not used since the plain Z-7987 is adequate for tracking objects to the limit of the instrument package.

Television Tracking

Analyses of various tracking methods have been reported previously (Reference 10). We will constrain this discussion to centroid tracking of point sources as required by the SPO.

A centroid tracker is an image integrating tracker. The video signal from the TV camera contains a complete description of the entire field of view (FOV) of the camera, (including that of target size, shape, shades of gray, etc.) to the limits of the capabilities of the camera. The entire field of view of the camera appears on the TV monitor but an adjustable size, movable gate reduces the sample area of the camera FOV to be used by the TV tracker to generate the error signals.

Centroid tracking integrates the video within the gate by partitioning the active gate area into a matrix. The centroid technique then processes any video information inside the tracking gate whose level exceeds a pre-set threshold level. The most

common centroid technique is one which determines the center of mass of the target.

The true centroid of a two dimensional object corresponds to its center of mass. By utilizing the x-y television scan and a high-speed horizontal clock, we may break each television frame into a matrix. The horizontal clock frequency is then calculated to provide a square matrix in the following manner:

$$\# \text{ of frames/second} = 30 \text{ Hz} \quad (9)$$

$$\# \text{ of lines/frame} = 525$$

$$\therefore \text{ the horizontal frequency} = 525 \times 30 \text{ Hz}$$

$$= 15.750 \text{ KHz}$$

$$= 63.5 \text{ } \mu\text{sec}$$

\therefore the horizontal clock frequency must equal

$$(525) (15.750) = 10 \text{ MHz}$$

$$= 100 \text{ nsec.}$$

Now we have a TV matrix with a square element of $64.0 \text{ } \mu\text{sec}$ vertically by 100 nsecs , horizontally. If we let this matrix element be defined as d_m , we have a representative element of mass which is continuously distributed over the x, y plane of the television frame. If we now let A represent the region over which d_m is distributed, we may calculate the center of mass

$$d_m = \delta(x, y) dydx = \delta(x, y) dA \quad (10)$$

where

$$\delta = \delta(x, y) \text{ is the density at the point } (x, y) \text{ of } A \quad (11)$$

the mass

$$(M) = \iint \delta(x, y) dA \quad (12)$$

the moment of mass with respect to the x-axis

$$M_x = \iint y \delta(x, y) dA \quad (13)$$

and the moment of mass with respect to the y-axis

$$M_y = \iint x \delta(x, y) dA \quad (14)$$

the coordinates of the center of mass (\bar{x}, \bar{y}) then becomes:

$$\bar{x} = \frac{M_y}{M} \quad \text{and} \quad \bar{y} = \frac{M_x}{M} \quad (15)$$

However, these are not convenient terms in which to implement a center of mass calculation with hardware. We must then redefine M , M_x , and M_y in more usable terms. The mass of the target is defined as the summation of all of the elemental masses (m)

$$M = m_1 + m_2 + \dots + m_n = \sum_{k=1}^n x_k m_k \quad (16)$$

In a corresponding manner, the moments of mass in the x and y axis may be determined:

$$M_y = x_1 m_1 + x_2 m_2 + \dots + x_n m_n = \sum_{k=1}^n x_k m_k \quad (17)$$

$$M_x = y_1 m_1 + y_2 m_2 + \dots + y_n m_n = \sum_{k=1}^n y_k m_k$$

Another centroid technique uses the information obtained from the multiple edge mode and operates on the four edge values. This is done by adding the leftmost coordinate of the target to the rightmost coordinate of the target and dividing by two. The result describes the center of the target in azimuth and the top and bottom edges

are processed to determine the elevation center. The disadvantage of this centroid technique is identical to the problem encountered in edge tracking. The edges used may represent false targets or random noise and the system will false lock or break lock.

The third most common centroid technique is an integrating technique similar to the first approach. The centroid of the image within the tracking gate is determined by dividing the tracking window into four quadrants, integrating the information within each of the four quadrants, and closing an internal loop such that the tracking gate is centered about the target with equal energy in each quadrant. The center of the gate now represents the centroid of the image. The disadvantage of this type of centroid processor lies in the internal loop that must be locked to balance the four-quadrant gate. The accuracy and response time of the centroid calculation is poor and often unstable.

Of the three centroid techniques discussed above, the first technique is the most accurate and versatile. It allows the target with the greatest mass to have the highest weighting factor in the centroid error signal determination.

Servo Interface

The error signals thus derived are then routed to the optional servo interface electronics within the automatic television tracker. Here a control signal is developed which is summed with the signal from the observer's stiffstick control in the SPO mount servo electronics. The tracker will produce a control signal only when a target image within the tracking gate is above threshold. The stiffstick will produce a control signal

only when the observer applies pressure to the stiffstick. Both contain integrator circuits which take 10 to 20 seconds to discharge.

In operation, the observer manually acquires the satellite using the stiffstick while guiding on the satellite through a guide telescope. An audio signal informs the observer when the satellite image is in the proper location for the instrument package. When the tracker thresholds on the satellite, the observer can sense the automatic system gradually take over and he can release the stiffstick. This system works very well in practice and was implemented without interfering with the critical SPO telescope mount tachometer feedback electronics.

Tracking Experiments

The PAGEOS satellite was tracked automatically on the nights of January 7, 1976 and January 11, 1976 as a test of the automatic television tracking system's capability to follow very slow satellites. The instrument package was activated during the January 7 experiments. The automatic TV tracking system provided smooth accurate tracks allowing the instrument package to operate with the smallest aperture (0.14 mr). Several stars were tracked also.

The PEGASUS I satellite was tracked on the night of January 22, 1976 as a test of the system's ability to track fast satellites. The PEGASUS I was acquired just above the horizon, tracked automatically through a maximum altitude of almost one radian and into shadow one-third radian above the opposite horizon. No controls on the TV tracker or camera were adjusted during the entire acquisition and tracking time. The track was smooth and accurate as before. In addition, several lighted aircraft were

tracked at rates far exceeding any existing satellite. Some of the moon's of Jupiter were tracked also.

Conclusion

The implementation of the Z-7987 image orthicon sensor and the DBA Series 606 Automatic Television Tracker provides a highly accurate automatic tracking capability for the Satellite Photometric Observatory. The 60 Hz sample rate provided by standard TV rates results in a smooth track with any satellite angular velocity. The sensitivity and non-blooming characteristics of the Z-7987 provides an excellent astronomical sensor which is almost photon noise limited. With one stage of intensification the tube would be photon noise limited at standard frame rates.

Acknowledgments

The work reported in this paper was supported by NASA/Langley under Contract NASL-13876. The author expresses thanks to Bob Lee and Dave McDougal of NASA/Langley and Forrest Diehl, Bill Hunt and Chet Bartusiak of Willey Research Labs for their assistance in refining the system design during the tracking experiments. The author especially thanks John Spalding of Los Alamos for his assistance in developing the camera system and sharing his experience with the Z-7987 image orthicon tube.

References

1. Lee, R. B. III and McDougal, D.S., "Vertical Ozone Profiles from Observations of Eclipsing Satellites," presented at the XVI Plenary Meeting of COSPAR, Akademie — Verlag, Berlin (1974).
2. Jensen, N., Optical and Photographic Reconnaissance Systems, John Wiley and Sons, Inc., New York, 1968, p. 17.
3. Schaff, F. L., "Television System Optimization for Astronomy and Special Applications," Proceedings of the S. P. I. E., Volume 44, (1974).
4. Janssens, T. J., "Theoretical Performance Figures for Low Light Level TV Cameras," Proceedings of the S. P. I. E., Volume 28 (1972).
5. Johnson, M. and Trapmore, C., "The Matching of Performance to Application for Low Light Level Television Systems," IEE Conference Publication No. 124, Low Light Level and Thermal Imaging Systems, Institution of Electrical Engineers, Savoy Place, London WC2 (1975).
6. Spalding, J. F., "A New S-25 Television Tube," presented at the Electro-Optical Systems Design Conference - 1971, Industrial and Scientific Conference Management, Inc., Chicago (1971).
7. Gurski, T. R. and Spalding, J. F., "Comparison of an Image Orthicon, Intensified — SIT, and Slow Scan SIT for Astronomical Acquisition," presented at the topical meeting on Imaging in Astronomy, Cambridge, Massachusetts, June 18-21, 1975.
8. Van Pelt, R., "TV Autotracking in RPV's," Electronic, Electro-Optic and Infrared Countemeasures, July, 1975 p. 47.

9. McDougal, D. S., Lee, R. B. III, and Romick, D.C., "Measured Physical and Optical Properties of the Passive Geodetic Satellite (PAGEOS) and the ECHO I," presented at the Symposium on the Use of Artificial Satellites for Geodessy, Washington, D.C., April 15-17, 1971.
10. Van Pelt, R., "System Applications of Automatic TV Trackers," presented at the Electro-Optical Systems Design Conference - 1975, Industrial and Scientific Conference Management, Inc., Chicago (1975).